

Selleri⁸ has pointed out, the c.m. energy of the secondary pions from the $\pi-\pi$ interaction would be such that in many cases a rescattering in the $(\frac{3}{2}, \frac{3}{2})$ state of one of these pions from the nucleon might occur. This might lead to the observed (π, N) Q -value peaks and the corresponding peaks in pion momentum spectra.

The principal kinematic features (momenta and Q values) observed in this and in other experiments¹⁶ at this energy are not necessarily indicative of the excitation of the $T=\frac{1}{2}$ resonance pion-nucleon states, since the momentum spectra of the recoil pion from $T=\frac{1}{2}$ isobar production and the decay pion from $T=\frac{3}{2}$ isobar production are expected to be similar. It thus appears unnecessary on the basis of the present evidence to invoke the postulated $T=\frac{1}{2}$ isobaric states to explain the observed effects, although excitation of these states is not ruled out. In view of increasing interest in theories involving π^* , K^* , and Y^* resonant systems³⁵ the experimental evidence for assuming more than one N^* state should be carefully examined.

It would seem that the kinematics of single neutral pion production in a limited sample, selected so as to avoid misidentification of the neutral particle, are in rather serious disagreement with the detailed predictions of charge states obtained from a simple isobar model which assumes the importance of $T=\frac{1}{2}$ nucleon isobars. On the other hand, the recoil nucleon energies

³⁵ H. P. Dürr and W. Heisenberg, *Z. Naturforsch.* **16A**, 726 (1961).

and the pion-pion energy distribution are consistent with the assumption that a strong pion-pion interaction initiates the reaction. The features of the angle and momentum distributions which suggest a strong pion-nucleon interaction might be qualitatively explained in terms of rescattering of the pions by the recoil nucleon in the $T=\frac{3}{2}$ pion-nucleon state. In view of the limited statistics of the experiment, no attempt has been made to calculate the pion-pion interaction cross section.

The selection technique for $(p\pi^-\pi^0)$ events which was used in this experiment appears to be a useful method for checking the results of pion-production studies in which other selection criteria are used. The number of events obtained with this method might be increased considerably if a larger bubble chamber could be used.

ACKNOWLEDGMENTS

We wish to thank the Alvarez Bubble Chamber Group of the University of California Lawrence Radiation Laboratory for their kindness in making the data of this experiment available. Dr. H. Bradner and Robert West provided invaluable assistance.

It is a pleasure to express our indebtedness to Professor J. G. Dardis for his contribution to the early phases of this work, and to Gunter Brunhart for many helpful suggestions. The assistance of Claudine Gall in scanning and analysis was invaluable. The cooperation of the University of Kentucky computing center is acknowledged with appreciation.

Multiple Meson Production in Proton-Proton Collisions at 2.85 BeV*

E. L. HART, R. I. LOUTTIT, D. LUERS,† T. W. MORRIS, W. J. WILLIS, AND S. S. YAMAMOTO

Brookhaven National Laboratory, Upton, New York

(Received December 1, 1961)

Measurements have been made on 753 four-prong events obtained by exposing the Brookhaven National Laboratory 20-in. liquid hydrogen bubble chamber to 2.85-Bev protons. The partial cross sections observed for multiple meson production reactions are: $pp \rightarrow (p+p \rightarrow p+p+\pi^+\pi^-)$, 2.67 ± 0.13 ; $pn \rightarrow (p+n \rightarrow p+n+\pi^+\pi^-)$, 1.15 ± 0.09 ; $pp \rightarrow (p+p \rightarrow p+p+\pi^0\pi^0)$, 0.74 ± 0.07 ; $d \rightarrow (p+n \rightarrow p+n+\pi^+\pi^-)$, 0.06 ± 0.02 ; four or more meson production, 0.04 ± 0.02 , all in mb. Production of two mesons appears to occur mainly in peripheral collisions with relatively little momentum transfer. In cases of three-meson production, however, the protons are typically deflected at large angles and are more strongly degraded in energy. The $\frac{3}{2}, \frac{3}{2}$ pion-nucleon resonance dominates the interaction; there is some indication that one or both of the $T=\frac{1}{2}, \frac{3}{2}$ pion-nucleon resonances also play a part. The recently discovered resonance in a $T=0$, three-pion state appears to be present in the $pp \rightarrow (p+p \rightarrow p+p+\pi^+\pi^-)$ reaction. Results are compared with the predictions of the isobaric nucleon model of Sternheimer and Lindenbaum, and with the statistical model of Cerulus and Hagedorn. The cross section for the reaction $\pi^0+p \rightarrow \pi^+\pi^-\pi^0+p$ is derived using an expression from the one-pion exchange model of Drell.

I. INTRODUCTION

THE scattering of nucleons by nucleons at high energies has been studied extensively in recent years. Such features of the interaction as the total and elastic cross sections have been investigated by experi-

mental groups using electronic counters.¹ However, this technique is of limited utility in its application to inter-

* Work performed under contract with the U. S. Atomic Energy Commission.

† Max Planck Institute, Munich, West Germany.

¹ F. F. Chen, C. P. Leavitt, and A. M. Shapiro, *Phys. Rev.* **103**, 211 (1956); B. Cork, W. A. Wenzel, and C. W. Causey, *Phys. Rev.* **107**, 859 (1957); M. J. Longo, J. A. Helland, W. N. Hess, B. J. Moyer, and V. Perez-Mendez, *Phys. Rev. Letters* **3**, 568 (1959); M. J. Longo, thesis, University of California Radiation Laboratory Report UCRL-9497, 1961 (unpublished); G. Von Dardel, D. H. Frisch, R. Mermod, R. H. Milburn, P. A. Piroué, M. Vivargent, G. Weber, and K. Winter, *Phys. Rev. Letters* **5**, 333 (1960).

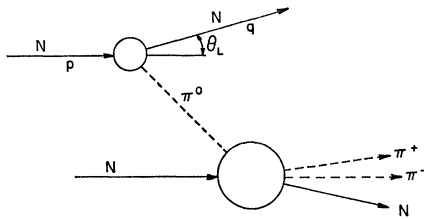


FIG. 1. Diagram for one-pion contribution to the reaction $p+p \rightarrow p+p+\pi^++\pi^-$. The quantities p , q , and θ_L are the initial and final momenta and the angle of scattering of the incident proton in the laboratory system.

actions resulting in more than two outgoing particles. Several proton-proton scattering experiments have been carried out in H_2 diffusion cloud chambers at energies sufficiently high (greater than 1.5 Bev) that the probability of producing two or more mesons is not small.²⁻⁴ These experiments obtained multiple meson production cross sections of 5 mb at 1.5 Bev, 17 mb at 2.75 Bev, and 17 mb at 5.3 Bev. However, the number of events available in each case was under 100 and the relatively low accuracy of measurement in these chambers caused considerable difficulty in identifying the reactions involved. Several measurements have also been carried out in emulsions.⁵

The advent of liquid hydrogen bubble chambers has made possible the detailed investigation of proton-proton interactions in the energy range above 1 Bev where the multiplicity of possible final states increases rapidly. The present paper reports on multiple meson production in p - p scattering at 2.85 Bev. In addition, experiments at 1.5 Bev⁶ and 2.0 Bev⁷ done with the Brookhaven 20-in. liquid hydrogen bubble chamber are in the process of analysis.

Much recent theoretical work has been concerned with multiple meson production in nucleon-nucleon collisions over a wide range of energies. Sternheimer and Lindenbaum⁸ have extended the isobaric nucleon model⁹ to include both the isotopic spin states $T=\frac{1}{2}$ (isobar masses $m=1.51$ and 1.68 Bev) and $T=\frac{3}{2}$ ($m=1.23$ Bev) of the pion-nucleon system. In this model it is assumed

that in the primary interaction the nucleon is excited to an isobaric state which subsequently decays into a nucleon and one or two pions.

Cerulus and Hagedorn¹⁰ have calculated multiplicities, charge state ratios, and pion spectra for multiple meson production using a generalized Fermi-type¹¹ statistical theory which includes the $\frac{3}{2}, \frac{3}{2}$ isobar channel. The phase-space integrals are evaluated by a Monte-Carlo method. The interaction volume is an adjustable parameter, which is taken to be independent of multiplicity. An assumption is made in this calculation that the matrix elements involved are all equal.

Drell¹² has extended the work of Chew and Low¹³ to obtain the one-real-pion exchange contribution to the inelastic nucleon-nucleon interaction from the principle that the transition amplitude has a pole close to the physical region for small scattering angles of the nucleon. From the diagram (Fig. 1), a formula is derived for the differential cross section for multiple meson production as a function of the energy loss and scattering angle of the recoil nucleon, the pion-nucleon coupling constant, and the total $\pi^0 p$ scattering cross section.

In this experiment, a study was made of proton-proton interactions involving four or more outgoing prongs. A list of the final states involved appears in Table I. Results on strange particle production¹⁴ and on two prong proton-proton scattering¹⁵ are reported separately. Multiple meson production involving two or more neutral outgoing particles can be separated as a group from the other events but cannot be analyzed because the number of constraints is insufficient.

TABLE I. Experimental cross sections for proton-proton interactions yielding four or six charged prongs.^a

Event type	Number	(mb)
$(pp+-)$	414	2.67 ± 0.13
$(pn++-)$	178	1.15 ± 0.09
$(pp+-0)$	115	0.74 ± 0.07
$(d++-)$	10	0.064 ± 0.020
2 neutrals (4 or more meson production)	2	0.013 ± 0.009
$(pp0), (\pi^0 \rightarrow e^+ + e^-)$ $(pn+0), (\pi^0 \rightarrow e^+ + e^-)$	23	0.15 ± 0.03
6 prong (4 or more meson production plus $(pp+-0), (\pi^0 \rightarrow e^+ + e^-)$)	5	$(0.024 + 0.008) \pm 0.014$
Total 4 or more meson production		$0.013 + 0.024 = 0.037 \pm 0.020$
Not measurable	11	

^a The errors indicated are statistical.

¹⁰ F. Cerulus and R. Hagedorn, CERN Report 5908/Th. 13 (1959).

¹¹ E. Fermi, Progr. Theoret. Phys. (Kyoto) **5**, 570 (1950); Phys. Rev. **92**, 452 (1953); **93**, 1434 (1954).

¹² S. D. Drell, Phys. Rev. Letters **5**, 342 (1960).

¹³ G. F. Chew and F. E. Low, Phys. Rev. **113**, 1640 (1959).

¹⁴ R. I. Louttit, T. W. Morris, D. C. Rahm, R. R. Rau, A. M. Thorndike, W. J. Willis, and R. M. Lea, Phys. Rev. **123**, 1465 (1961).

¹⁵ G. A. Smith, H. Courant, E. C. Fowler, H. Kraybill, J. Sandweiss, and H. Taft, Phys. Rev. **123**, 2160 (1961).

² W. B. Fowler, R. P. Shutt, A. M. Thorndike, and W. L. Whittemore, Phys. Rev. **103**, 1479 (1956).

³ M. M. Block, E. M. Harth, V. T. Cocconi, E. L. Hart, W. B. Fowler, R. P. Shutt, A. M. Thorndike, and W. L. Whittemore, Phys. Rev. **103**, 1484 (1956).

⁴ W. B. Fowler (private communication).

⁵ R. Cester, T. F. Hoang, and A. Kernan, Phys. Rev. **103**, 1443 (1956). W. M. Preston, R. Wilson, and J. C. Street, Phys. Rev. **118**, 579 (1960).

⁶ E. L. Hart, R. I. Louttit, and T. W. Morris (to be published).

⁷ E. Pickup, D. K. Robinson, and E. O. Salant, Bull. Am. Phys. Soc. **6**, 302 (1961); Phys. Rev. **125**, 2091 (1962); W. J. Fickinger, E. Pickup, D. K. Robinson, and E. O. Salant, Phys. Rev. **125**, 2082 (1962).

⁸ R. M. Sternheimer, and S. J. Lindenbaum, Phys. Rev. **123**, 333 (1961); Phys. Rev. Letters **5**, 24 (1960). *Proceedings of the 1960 Annual International Conference on High-Energy Physics at Rochester* (Interscience Publishers, New York, 1960), p. 205.

⁹ D. C. Peaslee, Phys. Rev. **94**, 1085 (1954); **95**, 1580 (1954); S. J. Lindenbaum and R. M. Steinheimer, Phys. Rev. **105**, 1874 (1957).

II. EXPERIMENTAL PROCEDURE

During the winter 1959-60, approximately 90 000 pictures were taken of 2.85-Bev protons passing through the Brookhaven 20-in. liquid hydrogen bubble chamber. The beam¹⁴ scattered from a carbon target in the Cosmotron and passed through a Hevimet Collimator and two 36-in. deflecting magnets to yield about 20 protons/pulse in the chamber. The momentum spread was calculated from the beam geometry to be 1.6% full width at half-height. The mean measured proton momentum in the chamber was within 1% of the Cosmotron energy calibration.

The bubble chamber was operated with a 0.8% volume expansion at 25.2°K. A light delay of 150 μ sec was used to take advantage of the short (10 μ sec) beam spill of the "rapid beam ejector."¹⁶ The chamber¹⁷ uses piston expansion and dark field illumination, and has a magnetic field of 17 000 gauss. Good temperature uniformity results in little turbulence and permits separation of pions from protons by bubble density measurement for momenta as high as 1.3 Bev/c.

A sample of 8669 of the best quality pictures was scanned twice for events with four or six outgoing prongs. A restricted acceptance region was chosen that included only about half the chamber volume in order that almost all outgoing prongs would be at least 15-cm long. The incoming protons were required to have a projected entrance angle within ± 2 deg of the beam average and to have a curvature not visibly differing from the other beam tracks. The initial momentum of all interacting protons was then taken to be the mean beam momentum. With the above restrictions, an average of one useful event per 10 pictures was obtained. Two independent scans each yielded 99% of the events observed in the other. The four- and six-prong events are probably the easiest ones to find in the pictures and the pictures used were of good quality. The scanning efficiency is estimated to be 98-99%.

Measurements were made on a six-times-life-size projected image with an automatic digitized measuring machine having an x - y stage motion with a least count of 1 μ . An effective setting error of about 4 μ on film was deduced from actual track measurements resulting in an error of 40 μ in space. Measurements of field free pictures indicate no serious turbulence or distortion in the chamber. Taking all effects into account, results indicate that a 1-Bev/c track 20-cm long can usually be measured with an error $\sim \pm 1.4\%$.

A series of programs for the IBM 704 was used to analyze the events. "TRED" determines spatial coordinates and calculates angles and curvatures of tracks. A kinematic analysis was done by "GUTS"¹⁸ which makes

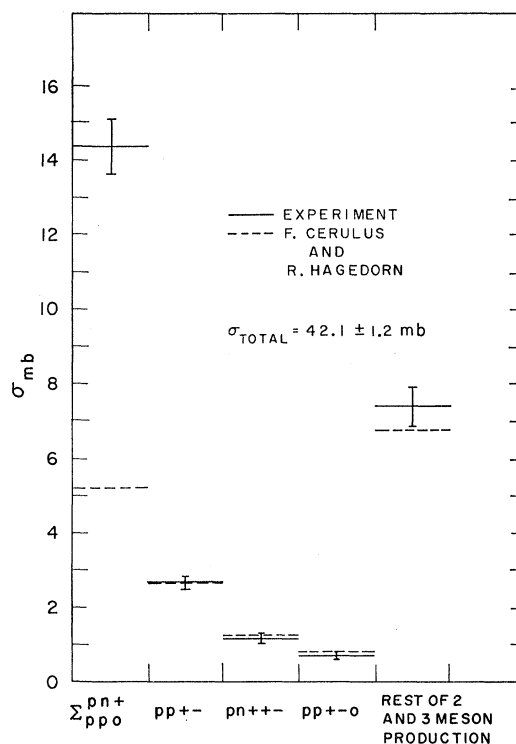


FIG. 2. Cross sections for one-, two-, and three-meson production. The dashed lines are the theoretical predictions of Cerulus and Hagedorn. The two curves are normalized for the reaction ($pp+-$). The ($pn+$) + ($pp0$) point is from the results of Smith *et al.*¹⁵

a least squares fit and obtains a χ^2 value from the amount by which the various track angles and momenta must be adjusted in order to obtain an energy and momentum balance for the type of event proposed. The four-prong events were fitted to the possibilities

$$p+p \rightarrow p+p+\pi^++\pi^-, \quad p+p \rightarrow p+n+\pi^++\pi^++\pi^-,$$

and

$$p+p \rightarrow p+p+\pi^++\pi^--\pi^0,$$

hereafter designated ($pp+-$), ($pn++-$), and ($pp+-0$), respectively. If these interpretations failed, trials were made for ($d++-$) and the events were inspected for Dalitz decay of a π^0 . Events with χ^2 values representing less than 0.04 probability were considered rejected from that particular category. The experimental χ^2 distribution for each interpretation then closely approximated the theoretical distribution for the appropriate number of constraints. The observed track bubble density of all events was required to be in agreement with that predicted by "GUTS" for the fit. This criterion made it possible in about 90% of the cases to remove the ambiguity of more than one possible fit for an event. In the remaining ambiguous cases, the interpretation with the smaller χ^2 was accepted.

Center of mass angles and momenta calculated by "GUTS" were punched by the program on cards for sorting. A third program punched information on Q values and angular correlations.

¹⁴ D. C. Rahm, Rev. Sci. Instr., **32**, 1116, (1961).

¹⁷ R. I. Louttit, *Proceedings of the 1960 International Conference on Instrumentation for High-Energy Physics* (Interscience Publishers, Inc., New York, 1961), p. 117.

¹⁸ J. P. Berge, F. T. Solmitz, and H. Taft, Lawrence Radiation Laboratory Report UCRL-9097 (unpublished).

TABLE II. Isobar model channels for four-prong events.

Channel	Threshold (Bev)	Mode of isobar decay		Final state
(a) $p+p \rightarrow 2N_1^*$	1.32	$N_1^* \rightarrow p+\pi^-$	$N_1^* \rightarrow p+\pi^+$	$pp+-$
(b) $p+p \rightarrow N_2^*+p_r$	1.32	$N_2^* \rightarrow N_1^*+\pi$	$N_1^* \rightarrow p+\pi$	$pp+-$
(c) $p+p \rightarrow N_1^*+N_2^*$	2.11	$N_2^* \rightarrow p+\pi^-$	$N_1^* \rightarrow p+\pi^+$	$pp+-$
(d) $p+p \rightarrow N_1^*+N_2^*$	2.11	$N_2^* \rightarrow N_1^*+\pi$	$2(N_1^* \rightarrow p+\pi)$	$pp+-0$
(e) $p+p \rightarrow N_1^*+N_2^*$	2.11	$N_2^* \rightarrow N_1^*+\pi$	$2(N_1^* \rightarrow N+\pi)$	$pn++-$
(f) $p+p \rightarrow 2N_2^*$	>2.85			

III. RESULTS AND DISCUSSION

A. Cross Section

In 8669 pictures scanned, a total of 753 four-prong events were found. Eleven of the events could not be measured for various reasons. The others are distributed among the charge states shown in Table I.

In addition, five six-prong events were found within the restricted region. These events are cases of four or more meson production, probably $(pp++--)$, with about a 25% calculated admixture of $(pp+-0)$ events in which the π^0 decays by the Dalitz mode.

The total interaction cross section at 2.85 Bev, combining the results of this experiment with references 14 and 15, has been measured to be 42.1 ± 1.2 mb, in good agreement with the value of 43.2 ± 0.4 found by Longo.¹ No reactions of the type $p+p \rightarrow p+p+K^+ + K^-$ were found in a sample of 6400 four-prong events.¹⁴

In Fig. 2 the cross sections for various final states drawn from this and the two-prong experiment¹⁵ are plotted together with the theoretical predictions of Cerulus and Hagedorn.¹⁰ Since the theory predicts only

relative cross sections, the theoretical points have been adjusted to force agreement with the measured $(pp+-)$ cross section, the best determined multiple meson process. The large discrepancy for one-meson production may be in part due to the implicit assumption in the theory of a central rather than peripheral interaction.

Sternheimer and Lindenbaum⁸ predict a value of 1.79 for the ratio $p+p \rightarrow (pn++-)/(pp+-0)$, in agreement with the experimentally determined 1.59 ± 0.27 . They expect a zero cross section for 4 or more meson production at 2.85-Bev kinetic energy; only 30 μ b is observed.

B. Kinematics of the Reactions $p+p \rightarrow (pp+-)$, $(pn++-)$, $(pp+-0)$

One of the most prominent features in inelastic nucleon-nucleon and nucleon-pion interactions at high energies is the $T=\frac{3}{2}$, $J=\frac{3}{2}$ pion-nucleon isobar. There is considerable evidence¹⁹ that the π^-p system has two additional resonances that may be interpreted as a pair of $T=\frac{1}{2}$ isobars with masses centered about 1.51 and 1.68 Bev. We shall consider in this section the possibility that multiple meson production in proton-proton interactions proceeds, at least in part, through the formation of such intermediate state isobars.

According to the isobar model developed by Sternheimer and Lindenbaum,⁸ the proton-proton interaction can proceed via any of a number of channels. The ones which can give rise to four-prong events are listed in Table II, together with the isobar decay modes and final state for each channel. The channel thresholds are calculated from the central mass of each isobar. In Table II, N_1^* represents the familiar $T=\frac{3}{2}$, $J=\frac{3}{2}$ pion-proton isobar, with mass $m_1=1.225 \pm 0.05$ Bev; N_2^* can be either of the pair of $T=\frac{1}{2}$, $J=?$ isobars with $m_2=1.51$ or 1.68 Bev²⁰; and p_r is the recoil proton in the two body reaction of channel (b).

With the simplest assumption of zero resonance width and no final state interaction, p_r has center-of-mass momentum of either 680 or 830 Mev/c, depending on which N_2^* isobar is excited.

It follows from the isobar model that the cross section

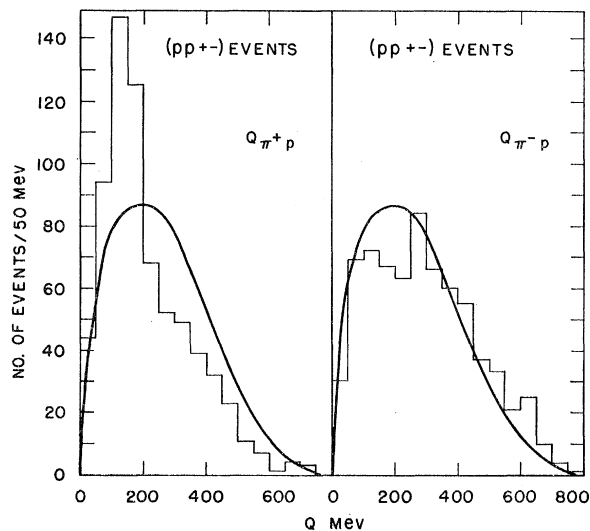


FIG. 3. Nucleon-pion Q -value distributions for the $(pp+-)$ events. The smooth curves are the predictions of the Fermi statistical model, normalized to the areas under the experimental curves.

¹⁹ A bibliography may be found in reference 8.

²⁰ The theory does not distinguish between them.

for the $(pp+-)$ reaction can be expressed as

$$\sigma(pp+-) = (1/5)\sigma_a + (5/9)\sigma_b + (1/2)\sigma_c, \quad (1)$$

where σ_a , σ_b , and σ_c are the cross sections for production in channels (a), (b), and (c), respectively; and the numerical coefficients are the statistical weights within each channel for the $(pp+-)$ mode of decay.

The presence of intermediate state isobars should be observable in the momentum, angle, and Q -value distributions of the final state particles. The measured (π^+p) and (π^-p) Q -value distributions for $(pp+-)$ events are plotted in Fig. 3, along with the predictions of the Fermi statistical model normalized to the same area. The Q value is defined as the sum of the kinetic energies of the two particles in their own center of mass system. The deviation from the statistical model due to the N_1^* resonance is clear in the Q_{p+} distribution, but the Q_{p-} histogram makes a reasonable fit to phase space. It does not show the peak at $Q \sim 150$ Mev that would be expected if the reaction $p+p \rightarrow (pp+-)$ proceeds principally by the formation and decay of two $T = \frac{3}{2}$ isobars, i.e., through channel (a).

On the other hand if channel (b) is excited, the decay of the N_2^* resonance should lead to a broad peak around 500 Mev in the (π^-p) Q -value distribution. Such a deviation from phase space is not convincingly indicated either.

In Fig. 4, the c.m. angular distribution of the protons from the reaction $(pp+-)$ is plotted on the left, and from $(pp+-0)$ and $(pn++-)$ on the right. The histograms of Fig. 5 give the c.m. momentum distributions of the protons from these reactions. Each $(pp+-)$ and $(pp+-0)$ event contributes two protons. The kinematic maximum proton c.m. momenta for two- and three-meson production are 1.020 and 0.932 Bev, respectively. The smooth curves are the theoretical

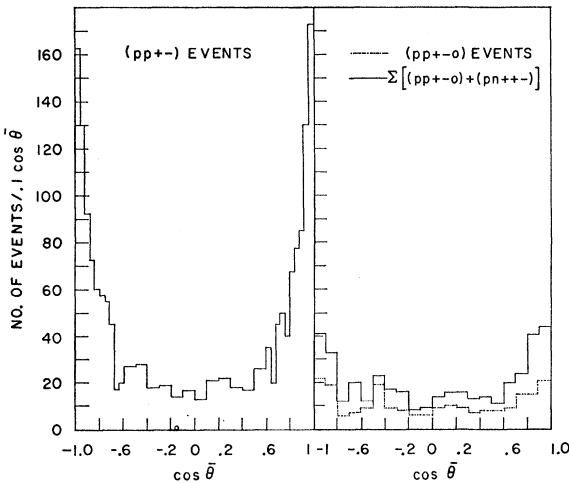


FIG. 4. Center-of-mass angular distribution of the protons from the reactions $(pp+-)$, $(pp+-0)$, and the sum of $(pp+-0)$ and $(pn++-)$. Two protons are contributed by each $(pp+-)$ and $(pp+-0)$ event.

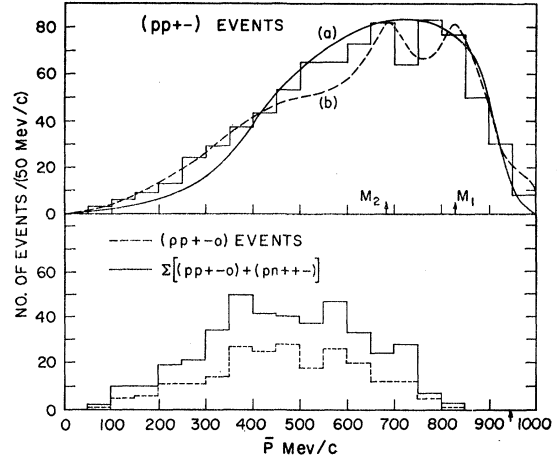


FIG. 5. Center-of-mass momentum distributions of the protons from the reactions $(pp+-)$, $(pp+-0)$, and the sum of $(pp+-0)$ and $(pn++-)$. The smooth curves on the upper figure are the isobar model predictions for the proton spectra for $2N_1^*$ [channel (a)] and N_2^*+p [channel (b)]. The two arrows are the theoretical spectrum peaks produced if channel (b) involves only one of the $T = \frac{3}{2}$ higher isobars. The arrow on the lower figure represents the maximum kinematically allowed momentum for three-meson production. The two-meson limit is 1020 Mev/c.

spectra predicted by the isobar model for channels (a) and (b), above. If there is no final state interaction, the momentum of the recoil proton, p_r , in channel (b) is uniquely determined by the mass of the isobar. Under the assumptions of zero width and no final state interaction, the two higher resonances result in momenta for p_r of 830 and 680 Mev/c, as indicated by arrows in Fig. 5. Channel (c) makes a poor fit to the $(pp+-)$ experimental curve and is not included.

From Figs. 4 and 5, there appears to be considerable difference in the kinematics of the protons from the two- and three-meson production events. The protons from the $(pp+-)$ reaction are strongly peaked forward and backward in the c.m. system, over half having $\cos\theta$ less than -0.8 or greater than $+0.8$. By comparison the three-meson production events are only mildly peaked. In the region $-0.8 < \cos\theta < +0.8$ the nucleons of all three reactions appear similar in both angle and momentum distribution. Outside this region the protons from $(pp+-)$ tend to have considerably higher c.m. momenta than the $(pp+-0)$ or $(pn++-)$ nucleons. The energy taken up by the extra π produced in the latter cases could explain in part the momentum shift, but the change in the angular distribution and the large magnitude of the momentum shift suggest that in two-meson production the protons are involved in a more peripheral collision, and that the dominant channels in two-meson production are different from those in triple production.

Relatively good agreement is obtained in Fig. 5 between the proton spectrum for $(pp+-)$ and the theoretical spectra for both channels (a) and (b). Unfortunately, the theoretical curves are too similar to permit, with the present experimental statistics, a reliable quantitative estimate of the relative importance

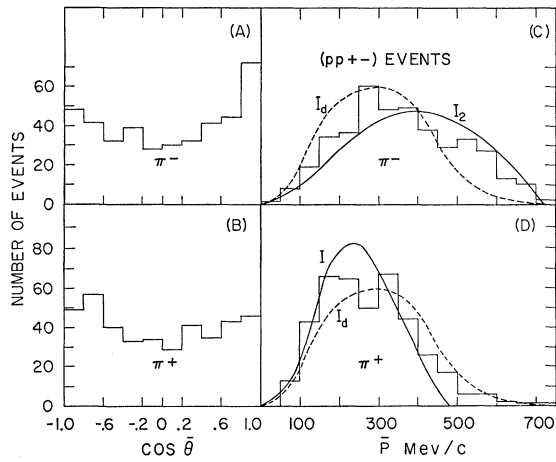


FIG. 6. Center-of-mass angular (A and B) and momentum (C and D) distributions of the pions from the reaction $(pp+-)$. The smooth curves are the momentum spectra predicted by the isobar model. I_d represents both π^+ and π^- in channel (a) while I_1 and I_2 are the theoretical π^+ and π^- spectra from channel (b). The kinematically allowed maximum momentum is 790 Mev/c.

of σ_a and σ_b . In an attempt to resolve this question, all the spectra were replotted separately for events having 2, 1, or 0 protons in the wings of the angular distribution, i.e., $|\cos \bar{\theta}| > 0.8$. The number of such events are in the ratio of 1.1:0.95:1.0, respectively. Results were inconclusive and indicated that either the c.m. angle of the protons is not strongly correlated with the channel taken by the event or that other processes than those of the isobar model are also involved.

The pion c.m. angle and momentum spectra from the $(pp+-)$, $(pn+-)$, and $(pp+-0)$ reactions are given in Figs. 6, 7, and 8, respectively. The angular distributions should all be symmetric about 90° in the c.m. system since the incident and target protons are identical. Within statistics the angular distributions satisfy this requirement, indicating the absence of

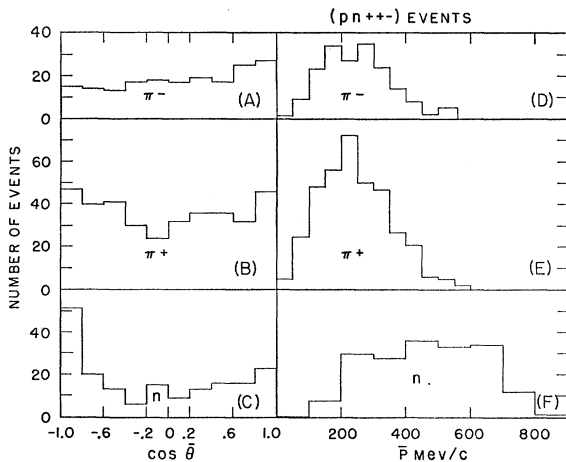


FIG. 7. Center-of-mass angular (A, B, and C) and momentum (D, E, and F) spectra of the pions and neutrons from the reaction $(pn+-)$. Each event contributes two pions to (B) and (E).

significant bias in the identification of individual particles.

In Fig. 6 the theoretical pion spectra for channels (a) and (b) of the isobar model are compared with the measured π^+ and π^- spectra for the reaction $(pp+-)$. The dashed curve I_d is the predicted c.m. momentum spectrum for both the π^+ and π^- mesons produced via channel (a). I_1 and I_2 are the pion spectra predicted for channel (b). I_1 represents the 90% π^+ , 10% π^- mixture from the decay of the N_1^* , while I_2 is the reverse combination from the N_2^* .

If channel (a) is dominant, the π^+ and π^- distributions should be identical. However, the statistical weights favor (b) by the ratio 25:9 (Eq. 1). The experimental momentum spectra do not look alike; the π^- being broader and tending to higher energy. Furthermore, the π^+ and π^- measured distributions each appear to fall about halfway between the two theoretical spectra proposed for the respective mesons, and do not agree well with either. The spectra from channel (c) again make a poorer fit and are not plotted. All this could

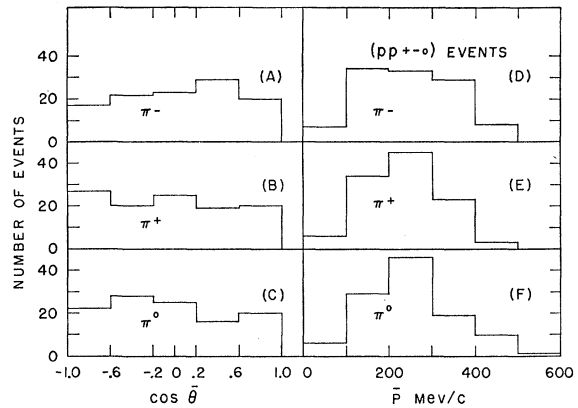


FIG. 8. Center-of-mass angular (A, B, and C) and momentum (D, E, and F) spectra of the pions from the reaction $(pp+-0)$.

suggest a mixture of states or perhaps a final state interaction.

For a reaction such as $N_2^* \rightarrow N_1^* + \pi^-$ where two close broad resonances plus the non-unique mass of the N_1^* would result in a confused (π^-p) Q -value distribution, it is possible to look for an interaction between a pion and nucleon by examining the distribution of the angle, θ_D , formed by the direction of motion of the pion in the c.m. system of the pion-nucleon pair, relative to the direction of motion of the c.m. of the pair in the event c.m. system (see Fig. 9). The distribution of θ_D will be symmetric about 90° if the pion and nucleon chosen are the products of the decay of some coupled system. This property is independent of the Q of the decay. The shape of this distribution is a more sensitive test of the existence of an interaction between the two particles than the distribution of the angle between their c.m. system momentum vectors. For Fig. 10, one

proton from each ($pp+-$) event is chosen by its having a (π^+p) Q value close to 150 Mev, to be the "isobar proton," i.e., the decay proton from the $T=\frac{3}{2}$ resonance. On the left hand side of Fig. 10 the θ_D distribution for the π^+ -“isobar proton” pair is plotted below the distribution of the π^+ -“other proton” pair. Since the proton was already selected by Q value, the lower curve is symmetric about $\cos\theta_D=0$ while the upper one is strongly backwards, indicating only that the correct “isobar proton” was chosen. On the right hand side, the distribution of θ_D formed by the same “isobar proton,” and the π^- is seen to be isotropic while the π^- -“other proton” combination is again peaked backwards, indicating that the π^- is frequently associated with the same proton as the π^+ . This is to be expected with the channel (b) reaction in which both π 's are emitted by the same proton.

From the above results, there is no doubt that isobars, at least the $T=\frac{3}{2}$ isobar, play an important role in multiple meson production. It also seems that there are considerable differences between the two and three meson production processes. The contribution to ($pp+-$) production from channel (c) appears to be

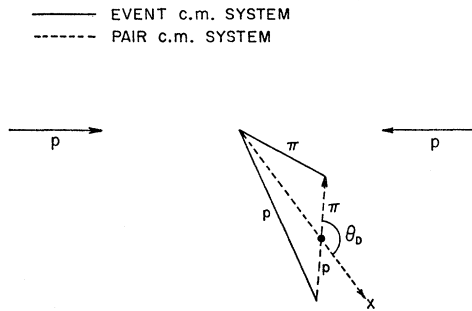


FIG. 9. Illustration of the angle, θ_D , formed by the direction of motion of the pion in the c.m. system of the pion-nucleon pair, relative to the direction of motion (X) of the c.m. of the pair in the event c.m. system.

small. Beyond that, it is not clear which of the first two terms in Eq. (1) dominates, in spite of the 25/9 weight factor in favor of the second. It would appear to be some mixture of the two. It is also possible that other processes, such as Fermi model production or final-state $\pi-\pi$ interaction may be present.

C. Q -Value Distributions

The results of the kinematic analysis of the four-prong events permit examination of a large number of possible combinations of two and three body final states. However, the final state configuration includes two nucleons and at least two pions, and the interactions may be quite complex.

The nucleon-pion Q -value distributions from the reaction $p+p \rightarrow p+p+\pi^++\pi^-$ have been discussed in Sec. B. The distributions from three-meson production events are shown in the histograms of Fig. 11. All the

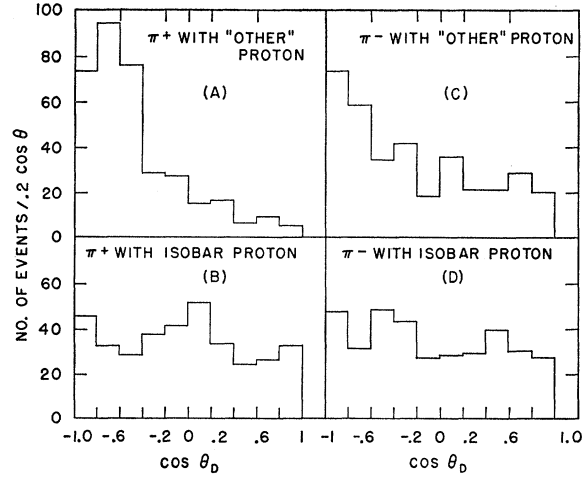


FIG. 10. θ_D distributions of the ($pp+-$) events. In (A) the histogram represents the angular correlation between the π^+ and the proton not in the $\frac{3}{2}, \frac{3}{2}$ isobar state. (B) is the π^+ , isobar proton pair. (C) and (D) represent the π^- angular correlations with the “other” and the isobar proton.

curves except the one at the far left are combined plots for a nucleon with each of two indistinguishable pions or a pion with each of two like nucleons. The $\frac{3}{2}, \frac{3}{2}$ resonance at $Q=150$ Mev dominates them all, and is sharpest for the pure $n\pi^-$ state. The maximum Q value allowed by the kinematics is 677 Mev.

In Fig. 12, the pion-pion Q -value distributions from the four-prong reactions are plotted. The smooth curve on the figure in the upper left hand corner represents the phase space Q -value distribution for the $\pi^+\pi^-$ pair from the reaction ($pp+-$).²¹ The maximum Q value allowed in this reaction is 817 Mev. For the others the maximum value is 677 Mev. The pion-pion resonance peak observed by Erwin *et al.*²² and Pickup *et al.*²³ in π^-p scatter-

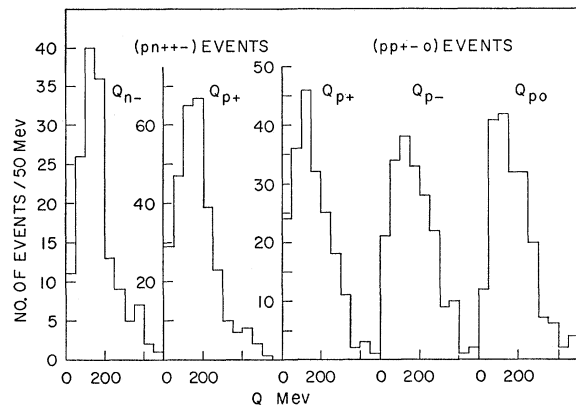


FIG. 11. Nucleon-pion Q -value distributions from the ($pn++-$) and ($pp+-o$) events. All histograms but the Q_{n-} are combined plots of a pion with each of two nucleons or a nucleon with each of two pions.

²¹ M. M. Block, Phys. Rev. **101**, 796 (1956).

²² A. R. Erwin, R. March, W. D. Walker, and E. West, Phys. Rev. Letters **6**, 628 (1961).

²³ E. Pickup, D. K. Robinson, and E. O. Salant, Phys. Rev. Letters **7**, 192 (1961).

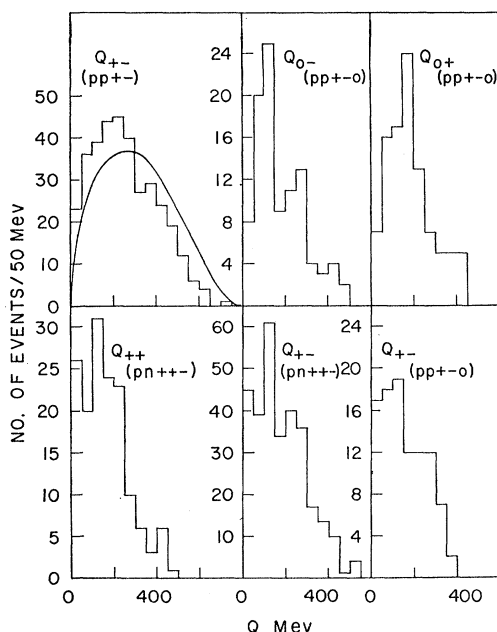


FIG. 12. Pion-pion Q -value distributions. The smooth curve superimposed on the Q_{+-} curve represents the phase-space distribution for the reaction $(pp+-)$.

ing and by Stonehill *et al.*²⁴ in π^+p scattering, at a Q of about 470 Mev, is not observed here. This can be explained if the interaction proceeds by a one-pion exchange with low momentum transfer, since in that case, the virtual pion can have energy only up to ~ 1 Bev, not enough to excite the $\pi\pi$ resonance. The Q distributions peak at low values and cut off well below the maximum allowed values, suggesting that most of the energy in the c.m. system is carried off by the two nucleons and that perhaps the pion-pion resonance is not excited.

The lower three distributions of Fig. 12 appear to have a large number of events with Q less than 50 Mev. This cannot be explained merely as a result of the production of three rather than two mesons, since the two upper right curves are also three-meson production and do not show the effect. Booth *et al.*²⁵ have reported what appears to be a strong s -wave $\pi\pi$ interaction in the $T=0$ state with an equivalent Q of about 20 Mev. If the deviations from phase space in Fig. 12 are real, the Q_{++} curve would indicate that the interaction also takes place in the state $T=2$. Clearly improved statistics are required here.

The three-pion final states from the reactions $(pn++-)$ and $(pp+-0)$ have, in general, a larger net kinetic energy in their c.m. system, i.e., a larger Q , than do the two-pion combinations from these reactions.

²⁴ D. Stonehill, C. Baltay, H. Courant, W. Fickinger, E. C. Fowler, H. Kraybill, J. Sandweiss, J. Sanford, and H. Taft, Phys. Rev. Letters 6, 624 (1961).

²⁵ N. E. Booth, A. Abashian, and K. M. Crowe, Phys. Rev. Letters 7, 35 (1961).

The three-pion, $T=0$, resonance observed by Maglić *et al.*²⁶ and Xuong *et al.*²⁷ in $\bar{p}p$ annihilation has a Q value of about 360 Mev, which is 110 Mev lower than that observed for the two-pion resonance. Thus the three-pion state falls well within the range of Q values observed here, and some further evidence of its existence is shown in Fig. 13. The Q values of 169 $\pi^+\pi^+\pi^-$ events (dashed line) and 106 $\pi^+\pi^-\pi^0$ events (solid line) are plotted in intervals of 20 Mev. The areas under both histograms have been set equal. A narrow spike is observed at a Q of 350 ± 10 Mev for the $\pi^+\pi^-\pi^0$ cases. Once again the statistics are poor but the probability of such a deviation occurring by chance at the appropriate energy is less than one in five hundred. The $\pi^+\pi^+\pi^-$ distribution appears flat, confirming that the resonance does not occur in the state $T=1$.

Several of the three-body Q distributions obtainable from the three-meson production events are of interest from the point of view of the isobar model. If these reactions proceed through an intermediate state as a $T=\frac{3}{2}$ isobar (N_1^*) and a $T=\frac{1}{2}$ isobar (N_2^*), as in channels (d), and (e), then in most cases $N_2^* \rightarrow p+\pi^-+\pi^0$ and $N_2^* \rightarrow n+\pi^-+\pi^+$ for the final states $(pp+-0)$ and $(pn++-)$, respectively. The Q values for these combinations should then peak at $Q=290$ or 460 Mev depending on which of the higher isobars is excited. The histograms of Fig. 14(A) indicate rather broad distributions which have their maxima about halfway between these two points. As in the case of the nucleon-pion Q -value plots, an additional indistinguishable pion or nucleon is present, so two values are obtained for each event. This increases the width of the distributions. Figure 14(B) is a plot of Q_{p++} from the $(pn++-)$ events, a $T=\frac{5}{2}$ state which cannot come from N_2^* . The bump in this curve, at ~ 300 Mev, could result if, in some of the events, the two π^+ mesons are both associ-

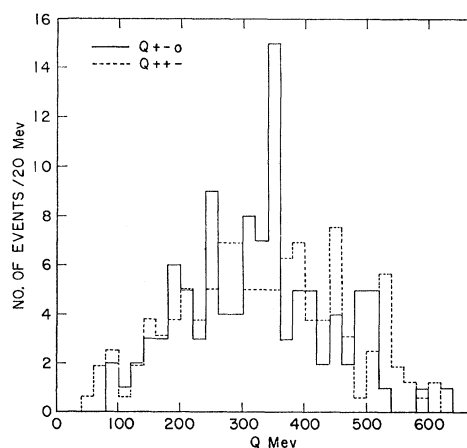


FIG. 13. Three-pion Q -value distributions from the reactions $(pp+-0)$ and $(pn++-)$.

²⁶ B. C. Maglić, L. W. Alvarez, A. H. Rosenfeld, and M. L. Stevenson, Phys. Rev. Letters 7, 178 (1961).

²⁷ N. H. Xuong and G. R. Lynch, Phys. Rev. Letters 7, 327 (1961).

ated with the same proton in the $\frac{3}{2}, \frac{3}{2}$ state, with each contributing ~ 150 Mev to the Q .

D. One-Pion Exchange Model

The one-pion exchange model proposed by Drell¹² (Fig. 1) leads to an expression for the differential cross section of the $(pp+-)$ reaction:

$$\frac{d^2\sigma}{dE_q d\theta_L}(E_p, E_q, \theta_L) = cf^2 \mathbf{F}(E_p, E_q, \theta_L) \sigma_{\pi^0}(E_{\pi^0}),$$

which is valid for small energy loss $E_p - E_q$, and small scattering angle θ_L , of the incident nucleon. f^2 is the pion-nucleon coupling constant and $\sigma_{\pi^0}(E_{\pi^0})$ is the total cross section for the reaction $\pi^0 + p \rightarrow \pi^+ + \pi^- + p$ as a function of energy $E_{\pi^0} = E_p - E_q$. Since the incident and target protons are indistinguishable in the final state, all the protons from $(pp+-)$ events satisfying $0.8 < |\cos\bar{\theta}| < 1$ (the protons in the "wings" of Fig. 4) are included in the calculation of σ_{π^0+p} . However, perhaps one-third of them are protons from the lower rather than the upper vertex of Fig. 1.²⁸ The final cross sections are multiplied by $\frac{2}{3}$ to correct for this contamination. An additional background from other production processes is estimated to be equal to the number of protons in the "wings" of the three-meson production

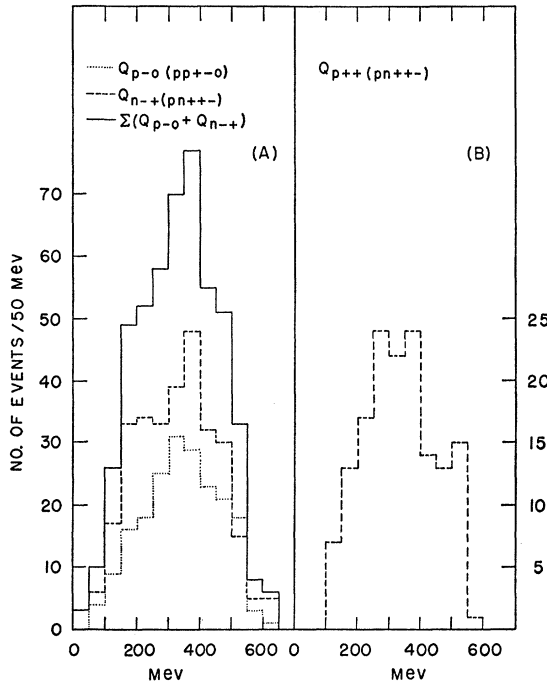


FIG. 14. Three-body Q -value distributions from the reactions $(pp+-0)$ and $(pn++-)$. Each event contributes twice to the Q_{p-0} and Q_{n-+} histograms.

²⁸ One half of the interactions considered here have one proton in the "wings," the other half have both. In each of the latter events, only one proton can be associated with the upper vertex of Fig. 1.

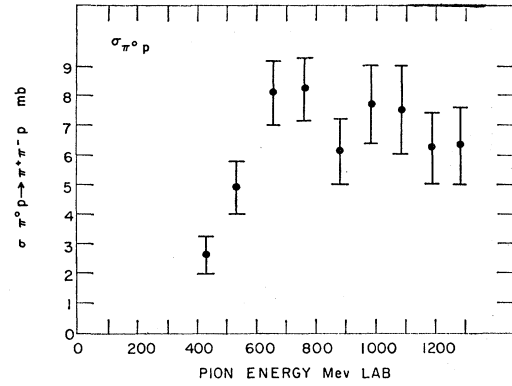


FIG. 15. The $\pi^0 p$ cross sections as a function of pion energy obtained from the Drell analysis of the $(pp+-)$ events. Corrections indicated in section D are made for background due to other processes.

proton angular distributions and is subtracted. The remaining events are averaged over 50-Mev/ c intervals and the differential cross sections, $(d^2\sigma/dE_q d\theta_L)$, are obtained. The expression $cf^2 \mathbf{F}(E_p, E_q, \theta_L)$ is transformed to the c.m. system and averaged over the same 50-Mev/ c intervals for $0.8 < |\cos\bar{\theta}| < 1$. A division of the measured cross sections by the corresponding values of the expression thus obtained yields σ_{π^0+p} as a function of energy (Fig. 15). The dip in cross section at ~ 850 Mev is generated by the dip in the proton momentum spectrum, and is no more significant statistically than the latter (see Fig. 5). As E_{π^0} (i.e., $E_p - E_q$) approaches 1 Bev, the requirement of a small energy transfer is not satisfied and the significance of the cross section curve in that region becomes questionable. At the lower energies the cross sections of Fig. 15 are consistent with those obtained from charge independence.

In the above discussion the $\pi^0 p$ cross section was obtained from the proton momentum distribution after averaging over the proton angular distribution between 0.8 and 1 in $|\cos\bar{\theta}|$. Conversely, the detailed proton angular distribution, averaged over proton momenta between 600 and 900 Mev/ c may now be derived from the $\pi^0 p$ cross section and compared with the measured distribution. This result is presented in Fig. 16. Since σ_{π^0+p} has been obtained from the $|\cos\bar{\theta}| > 0.8$ data, the curve and the histogram will, if integrated over that region, give the same area. Once again, as the angle increases, the requirements of the theory are not satisfied and the agreement is poorer. However, even in the region where the conditions are satisfied, near $|\cos\bar{\theta}| = 1$, the slopes of the curves differ.

IV. CONCLUSIONS

There is no doubt that the $\frac{3}{2}, \frac{3}{2}$ resonance plays a strong part in nucleon-nucleon interactions. It shows up in all the reactions observed in this experiment and constitutes a striking departure from a purely statistical interaction. There is some indication that the higher

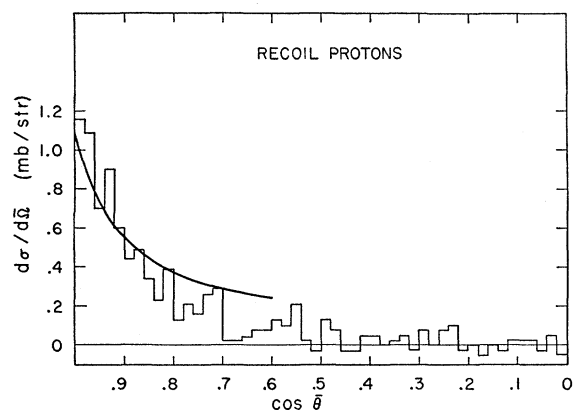


FIG. 16. Differential cross section for recoil protons with c.m. momenta between 600 and 900 Mev/c. The solid curve represents the experimental distribution for $(pp+)$ events with 0.050 mb/sr subtracted for background. The smooth curve is derived from the $\pi^0 p$ cross section of Fig. 15.

pion-nucleon resonances may contribute to the interaction, but it is not clear which of the possible modes of the multiple isobar model dominates, two and three meson production. It appears unlikely that this model gives a full description of the process.

It is also possible that the $T=0$ three-pion resonance, (the ω^0) and perhaps some pion-pion interaction at a $Q < 50$ Mev are present. However, they are not strong

and improved statistics are required to establish them with certainty.

Smith *et al.*¹⁵ have shown that p - p interactions producing a single meson are mostly peripheral collisions with little momentum transfer. This is also true for the production of two mesons, but three-meson production appears to involve more central interactions in which the nucleons typically give up a large part of their energy to the pions.

The cross section for $\pi^0 + p \rightarrow \pi^+ + \pi^- + p$ obtained from the Drell formula appears reasonable, at least at low incident pion energies, but to obtain the necessary statistics, his limits on the energy loss and scattering angle of the incident proton have not been strictly satisfied, which may explain the difficulties in attempting to predict the detailed proton angular distribution.

ACKNOWLEDGMENTS

The authors wish to thank the Cosmotron Department and the many members and guests of the Brookhaven Bubble Chamber Group who assisted in this experiment. Thanks are due also to R. M. Sternheimer and G. C. Wick for stimulating discussions and to the Yale Group for providing their results prior to publication. We are grateful to B. Zorn for checking the cross section for production of deuterons in this experiment.